

# A comparison of transient and conventional approaches to AMT

David Goldak <sup>1</sup> and Peter Kosteniuk <sup>2</sup>

<sup>1</sup> *EMpulse Geophysics Ltd. (empulse@sasktel.net)*

<sup>2</sup> *Kosteniuk Consulting Ltd. (kostp@sasktel.net)*

---

## Abstract

The natural electromagnetic field in the frequency range above 1 Hz is predominantly due to lightning discharges. The random, incoherent sum of globally distributed sources gives rise to a low level quasi-continuous component which is, in general, elliptically polarized. The effects of discrete events related to individual lightning discharges from either relatively nearby and/or very large current moment discharges are superimposed on this continuous component. 'Nearby' in this context is defined relative to the scale of global waveguide attenuation, which at 100 Hz is of the order of 5000 km whilst at 5000 Hz it is perhaps more like 1500 km.

The transient event signals can be much larger amplitude than the background component, but they are also strongly linearly polarized. The diversity of the polarization affects the stability with which Earth response curves can be estimated.

A 'transient' approach to AMT involves the time localized recording of linearly polarized transient event signals. Although not widely adopted, this is not a new approach, having been used previously by many others, including Don Hoover of the USGS in the 1970's, Keeva Vozoff, Ken Paulson and Andreas Tzanis in the 1980's, and Stephen Garner in the late 1990's.

The use of linearly polarized transients with conventional estimation procedures such as remote reference (RR) produces a bias that is additional to that caused by finite signal-to-noise ratio (SNR) and sample size. To improve the transient approach, we have developed a data processing algorithm called Adaptive Polarization Stacking (APS) that is specifically designed to work with linearly polarized transients. This new method produces results which properly reflect the polarization diversity, SNR and sample size in the final Earth response curves and error bars. We have shown that our APS algorithm has a higher order bias convergence than RR when applied to transients with typical polarization characteristics.

In this paper, we compare results obtained with conventional and 'transient' AMT data collected on the same seismic line by survey crews that were in the survey area at the same time.

Despite our first generation coils being at least four times noisier at low frequency and ten times noisier at high frequency than those used by our conventional survey colleagues, and that our 12 bit analog-to-digital-converter (ADC) (c/f the 24 bit ADC used in the conventional survey) had a software bug that required the removal of all of our pre-trigger data, we believe that our impedance data turned out as good as our colleague's in terms of curve smoothness and width of dead-band, and that our tipper data is demonstrably better.

## Introduction

The Mesoproterozoic Athabasca Basin (AB) in northern Saskatchewan, Canada, consists of flat lying terrestrially-derived sediments that exceed 1 km thickness in places. The AB rests unconformably on crystalline basement rocks which are generally comprised of felsic gneiss, metavolcanic rocks and graphitic pelitic schist. Typical exploration practice is to use electromagnetic methods to map graphitic shear zones (i.e., basement conductors) and subsequently carry out DC resistivity surveys to search for alteration halos in the sandstone above the basement conductors. The goal is to find areas of increased fluid flow and therefore possibly areas of uranium deposition (Leppin and Goldak, 2005). However, recent 'transient' AMT surveys have shown the ability to map conductive sandstone alteration with resolution comparable to DC resistivity (Powell et al., 2007; Nimeck and Koch, 2008).

As part of a multi-disciplinary study ('EXTECH IV'), an audio magnetotelluric (AMT) survey was carried out in the Shea Creek area, less than 15 km south of the formerly producing Cluff Lake mine, Athabasca Basin region of northern Saskatchewan (Craven et al., 2007) (Figure 1). Although not formally a part of the EXTECH IV program, the authors were given the opportunity by AREVA Resources to survey seismic line WAS-4 with their transient AMT equipment. This paper deals with the two AMT data sets collected on this line where a relatively direct comparison can be carried out of the results (i.e., those obtained using a transient approach by the authors, and those obtained using the more conventional approach in a survey performed by a different service provider). Reflection seismic, gravity, DC resistivity and UTEM III fixed loop surveys have also been completed on WAS-4.

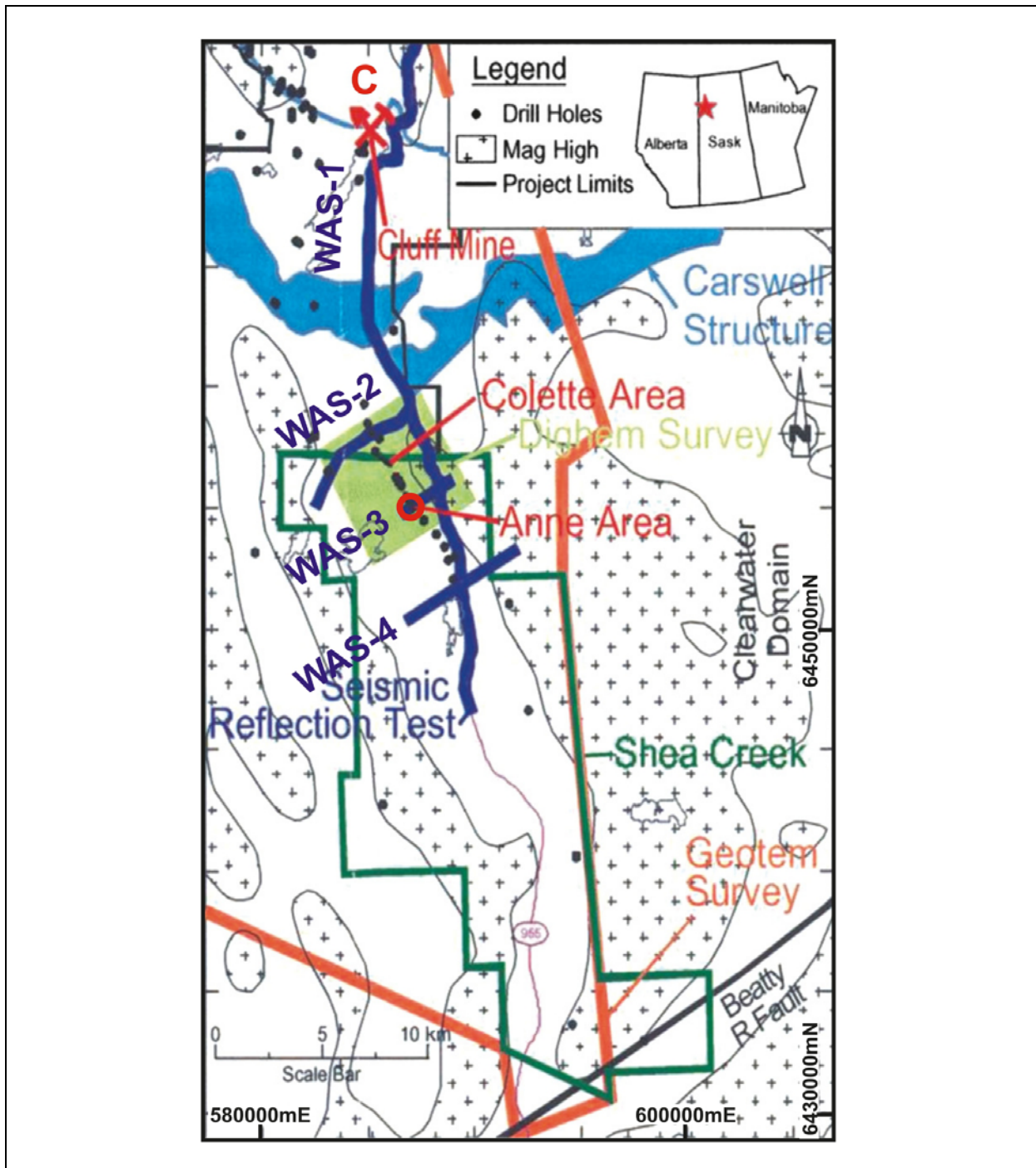


Figure 1. Location map for the survey area, courtesy of Hajnal et al. (2010).

## Transient and Conventional AMT

The natural electromagnetic field in the frequency range above 1 Hz is predominantly due to lightning discharges, the energy from which is partially trapped within the Earth-ionosphere waveguide. The natural field can be considered as having two components; a transient component due to individual lightning discharges, and a low-level background component due to the random, incoherent sum of global activity. It is estimated that there are of the order of 50 lightning discharges per second (Kotaki and Katoh, 1983). Global waveguide attenuation is such that the continuing component is most significantly present at frequencies in the range of approximately 7 to 200 Hz, and to a lesser degree from 7,000 to 15,000 Hz, i.e., these are the frequency bands in the ELF/VLF range (i.e., ELF – 3 Hz to 3 kHz, VLF – 3 kHz to 30 kHz) where global waveguide attenuation is less than 3 dB/1000 km (Barr, 1970).

To enhance data quality, especially outside of these frequency ranges, we take a ‘transient’ approach to AMT. Namely, the time localized recording of individual transient events, so called ‘sferics’, from individual lightning discharges. This is not new and has been done by many others, including Hoover et al. (1976), Tzanis and Beamish (1987), Kosteniuk and Paulson (1988), Vozoff (1991) and Garner and Thiel (1999).

This is contrasted with conventional AMT practice which is to extract information related to the background continuous signal assuming a constant influx of energy. While the source field is to a good approximation continuous in certain frequency ranges, significant enhancement of signal-to-noise ratio (SNR) is afforded by recording the transient component in a time localized fashion (Figure 2).

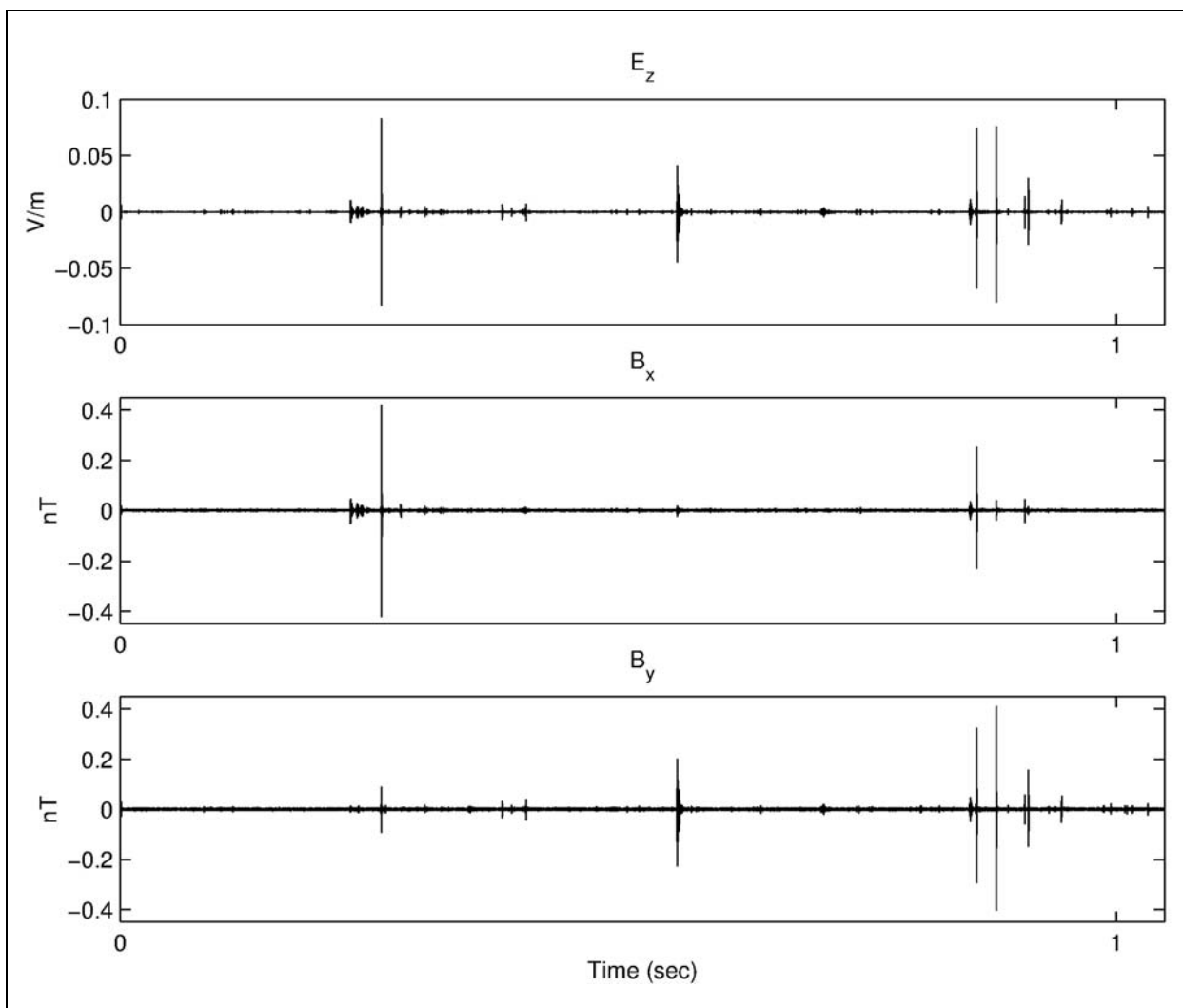


Figure 2. Time series record of electric and magnetic field signals illustrating the presence of discrete, high amplitude events.

The rate at which these discrete events are present depends on location and season. For example, it has been our experience in high northern latitudes during winter that the rate of arrival of useful events may be as little as one or two per minute, and consequently, a short continuous recording of several seconds is unlikely to contain any useful transients.

The transient events are strongly linearly polarized, the polarization diversity of which affects the accuracy of estimated Earth response curves (i.e., the level of bias in the solution). If we consider a scatter plot of two events (Figure 3), the angle between events is akin to specifying the condition number of the pairs of simultaneous linear equations involved in the estimation of the impedance tensor and/or tipper. A narrow angle produces a large condition number and an unstable system, whilst a wider angle increases stability, with 90 degrees between events being ideal. The stability of the linear system, as partly dictated by the angle between events, produces a bias additional to that caused by finite SNR and finite sample size (Goldak and Goldak, 2001).

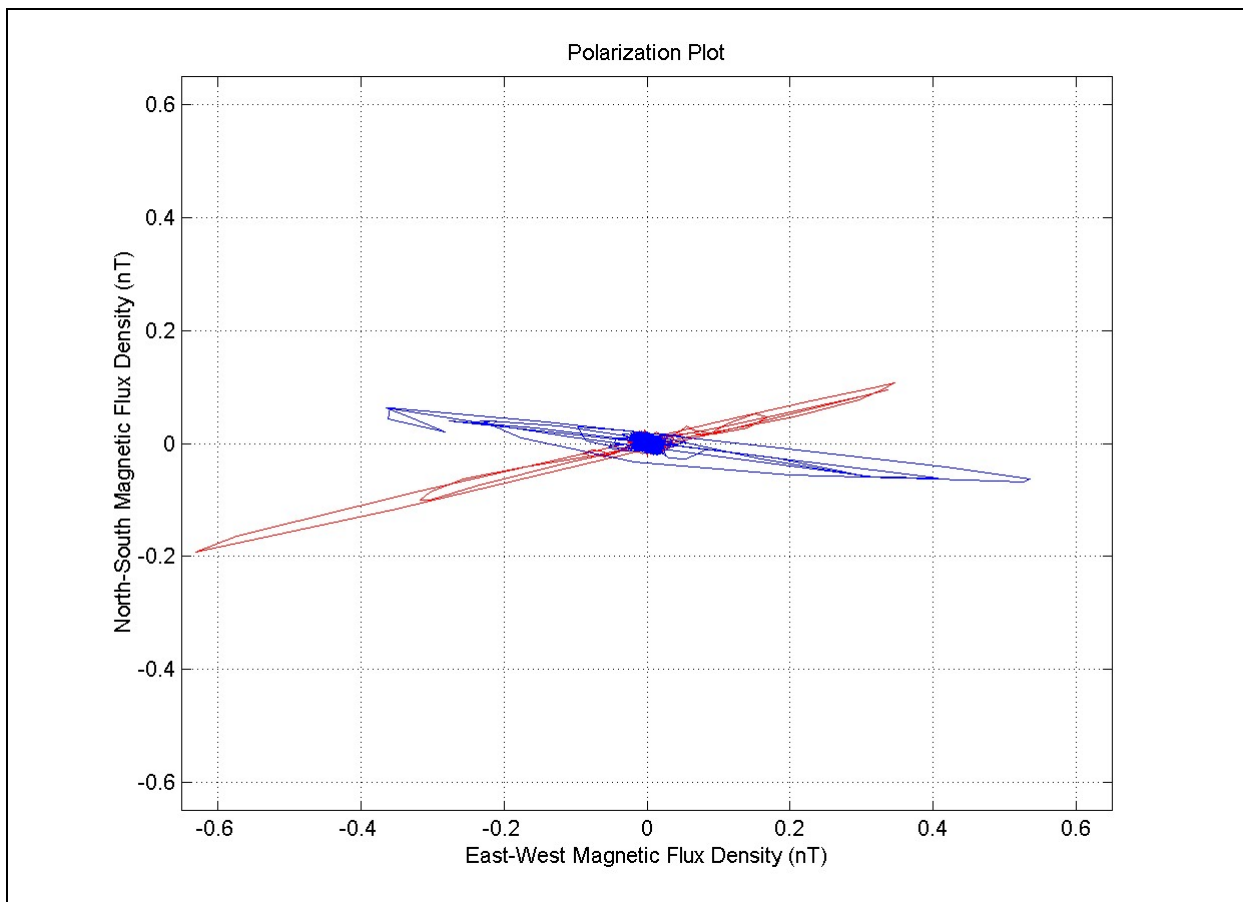


Figure 3. Scatter plot illustrating the strong polarization present in the signals from individual events.

This situation was the motivation behind the development of our Adaptive Polarization Stacking (APS) algorithm. We sought a method that can detect and 'adapt' to the diversity of polarization of the linearly polarized (transient) data, SNR and sample size, and one that communicates the stability of the linear system involved through the final Earth response curves and error bars.

A key feature of APS is the ability to enhance the SNR, to an extent, through a time-domain averaging of the transients. High quality estimations of impedance and tipper are then possible, even with narrow angle sources. An example of the stacking process is shown in Figure 4 where we note that peak-to-peak signal amplitude has been increased by approximately a factor of twenty after thirty-eight averages.

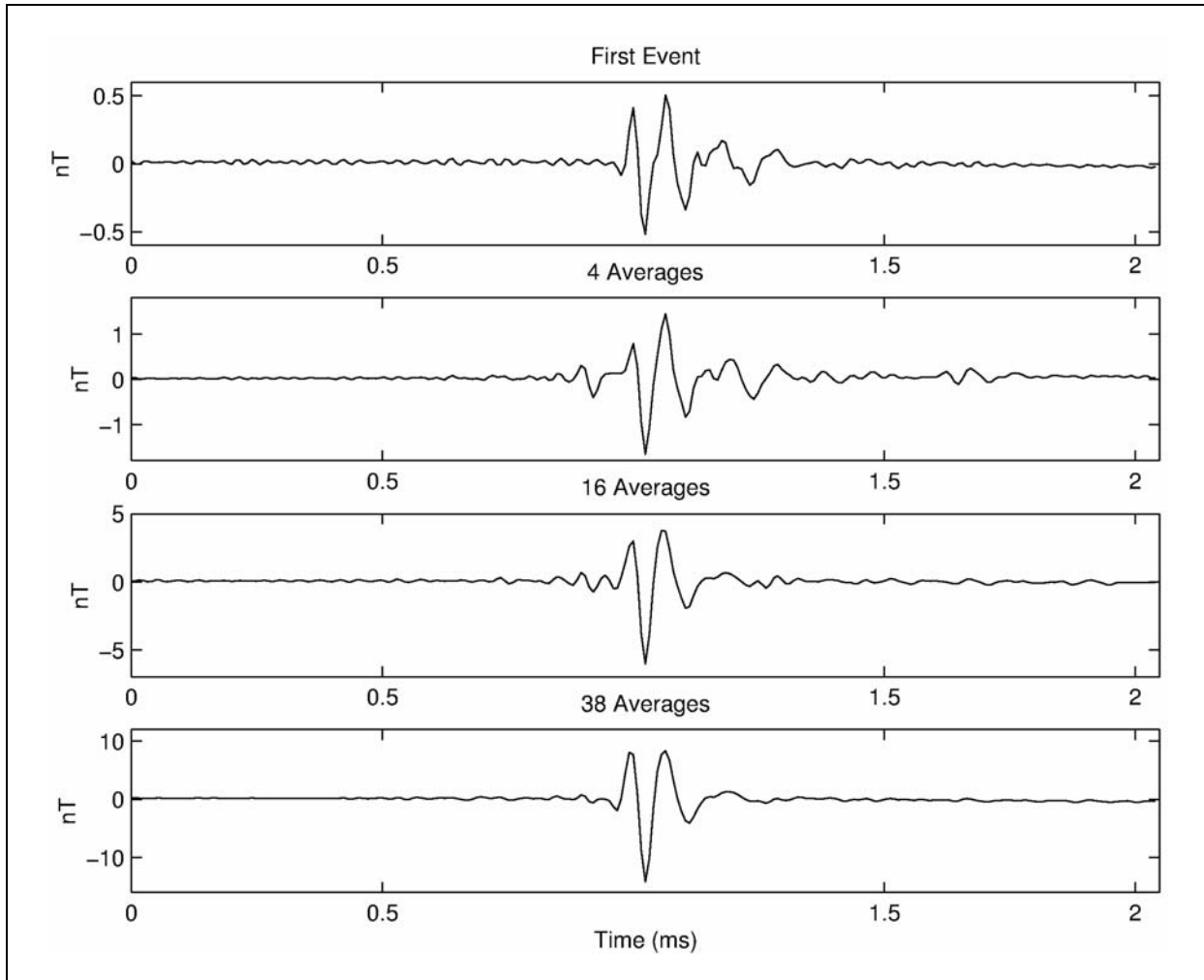


Figure 4. Time series magnetic field results for increasing levels of stacking.

Even though some fine-scale signal cancellation occurs due to non-similarity of time-domain waveforms, our belief is that extensive Monte Carlo analysis of bias and error bar capture indicates that APS provides the greatest benefit of bias reduction and precision of data (i.e., error bar size and error bar capture of true curve), making it the preferred approach for processing transient data. Many different algorithms have been tested, including what we called 'curve-stacking' whereby multiple impedance and tipper estimates were obtained from unique, multiple pairs of events and the curves stacked in a weighted sense, either with one single weight per curve or with frequency dependent weights across each curve. Even though the "curve-stacking" technique has absolutely no signal cancellation, APS still provides a far greater benefit in terms of accuracy (i.e., level of bias, error bar size, error bar capture), especially for the diagonal elements of the impedance tensor 'Z' and the secondary tipper component, both of which are very important for 3D inversion.

Many different weighting/stacking schemes have also been tested with APS and in the end, it would seem to us that ensuring maximum noise cancellation is the most important consideration, even if that means accepting some fine scale signal cancellation. We have further shown that, given transients with typical polarization characteristics, our APS algorithm has a higher order bias convergence than remote referencing methods (Goldak and Goldak, 2001).

### Survey parameters and results

Survey coverage at Shea Creek is shown in Figure 5, with seventeen 'conventional' AMT stations and thirty-six 'transient' AMT stations. Only those stations jointly occupied will be compared. A right handed co-ordinate system was used, with the positive x-axis direction being perpendicular to the survey line direction (327°), the positive y-axis direction being parallel to the survey line (57°), and the

positive z-axis being downwards. Table 1 provides a summary of the acquisition and processing parameters of the two survey methods. The estimated resistivity/phase results are shown in Figure 6 whilst the tipper results are shown in Figure 7.

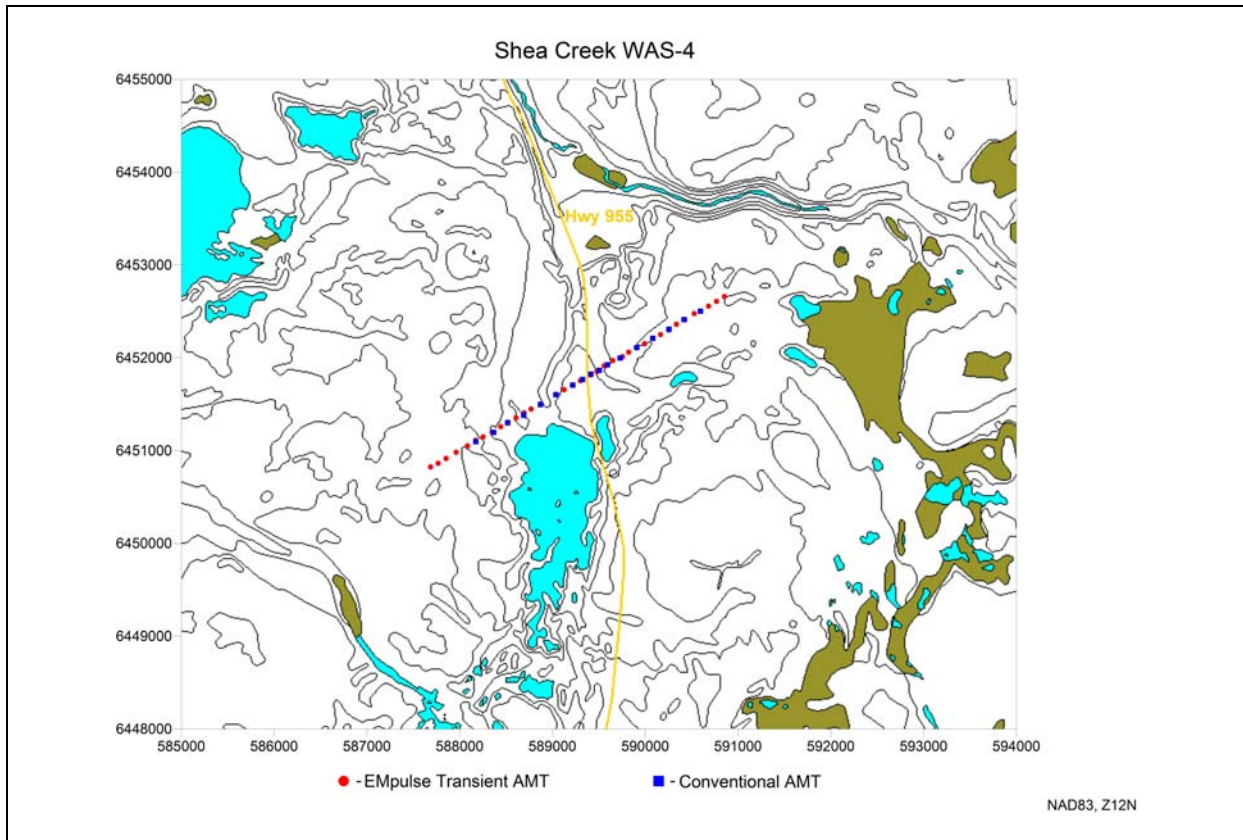


Figure 5. AMT station coverage for the Shea Creek Survey.

Table 1. Summary of AMT survey parameters.

	Transient	Conventional
<b>Recording Method</b>	Threshold triggered one second bursts, pre-trigger data (0.25 s) discarded due to an ADC driver bug, 20 minute typical recording length.	Continuous 7 minute recording for $f < 1000$ Hz, continuous 7 s recording for $f > 1000$ Hz
<b>Data Bandwidth</b>	5 Hz to 32 kHz	8 Hz to 20 kHz
<b>Sample Rate</b>	125 kHz	2048 Hz for $f < 1000$ Hz, and 4096 Hz for $f > 1000$ Hz
<b>ADC Resolution</b>	12-bit	24-bit
<b>Induction Coils</b>	First generation GRG-1, negative field feedback, noise floor of 9 fT per root(Hz) at 1000 Hz, secondary resonance (shielding) issues (see Figure 9).	EMI BF-6 (current-voltage converter style ?), advertised noise floor of 1 fT per root(Hz) at 1000 Hz (see Figure 9).
<b>Electric Field</b>	Lead-Lead-Chloride porous pot electrodes with 100 m separation.	Stainless steel stakes with 50 m separation.
<b>Data Processing Algorithm</b>	Adaptive Polarization Stacking	Robust remote-reference
<b>Analog signal conditioning</b>	Yes	No

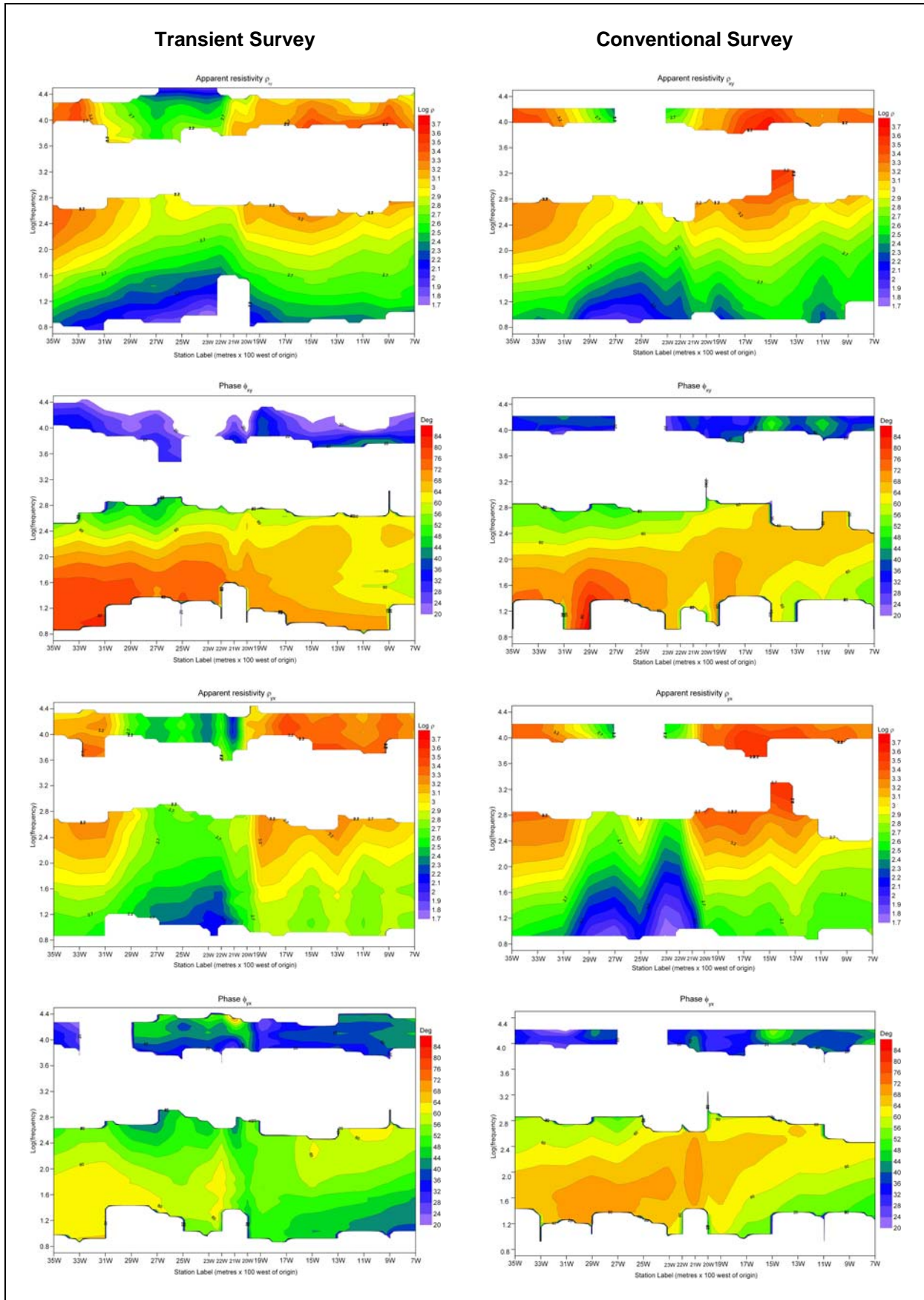


Figure 6. TE mode (xy) and TM mode (yx) apparent resistivity and phase results.

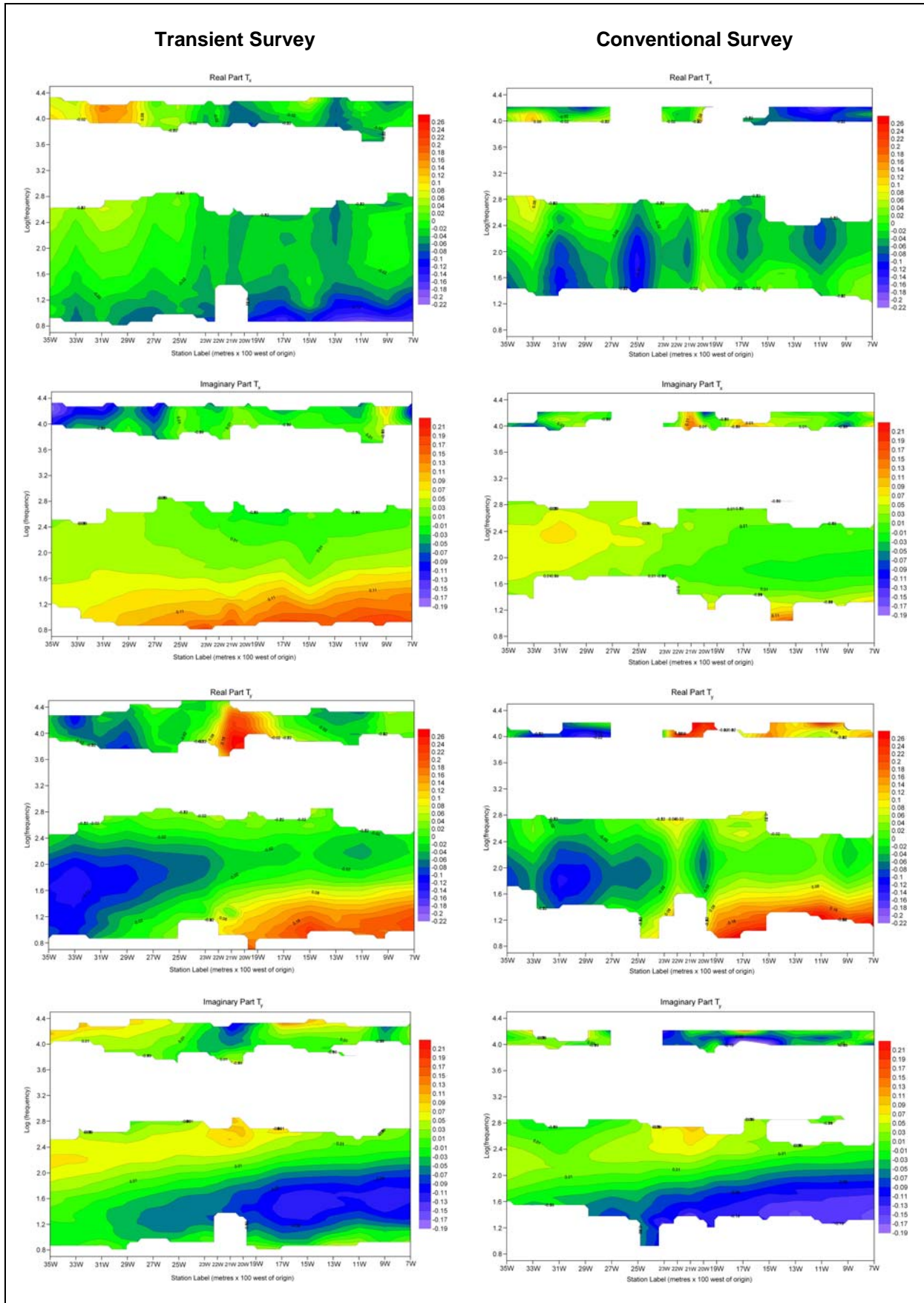


Figure 7. Tipper results.

## Discussion

The APS estimates shown in Figure 6 and Figure 7 use a constant frequency vector with 15 points-per-decade. Conversely, the robust RR code (Larsen et al., 1996) outputs a variable length frequency vector which depends on data quality with respect to bandwidth. For the sake of plotting and subsequent 2D inversion (i.e., interfacing with our software), a simple linear interpolant was used to interpolate the conventional robust remote-reference estimates to the constant APS frequency vector. Blank areas of the plots indicate frequencies for which the codes produced bad data.

With respect to the resistivity and phase data, the APS estimates are significantly more 'bi-modal' in that the TE mode (xy) and TM mode (yx) APS estimates show significant differences whilst the robust RR estimates produce very similar TE and TM mode estimates, especially with respect to the phase. Compared to the robust RR estimates, the TE mode APS results are spatially broader and smoother whilst the TM mode APS results are more sharply varying. The largest discrepancy between APS and robust RR estimates is with the TM mode (yx) phase (i.e., the bottom pair of plots in Figure 6).

Despite the fact that the GRG-1 coils were ten times noisier at high frequency (Figure 8), the high frequency APS resistivity estimates are as good as or better than the conventional estimates. The shallow alteration zone is better seen in the TE mode APS estimates (i.e., the upper two sets of plots in Figure 6), and evidence of a lateral contact is clearly seen in the TM mode APS estimates between stations 20W and 21W (i.e., the centre of the lower two sets of plots in Figure 6).

The APS high frequency phase estimates were unfortunately corrupted by secondary resonance issues due to inadequate electro-static shielding of our first generation coil. The width of the dead band at about 2 kHz is very similar between the two systems, despite our GRG-1 coil being ten times noisier than the BF-6 coils used on the conventional survey above 1 kHz (Figure 8).

With respect to the tipper data, higher quality estimates are seen with the transient data which shows a higher degree of self consistency and wider bandwidth. A clear low frequency crossover on  $T_y$  is evident in the vicinity of 23W which also corresponds to the regions of lowest resistivity seen in the xy and yx apparent resistivity data. In agreement with the TM mode APS estimates, a high frequency tipper anomaly occurs at 20W/21W ( $T_y$ ) which is further indicative of the lateral contact there. Interestingly, the western edge of the contact in the vicinity of 29W produces more of a  $T_x$  anomaly (VLF range), and therefore may be more oblique to line than the contact at 20W/21W.

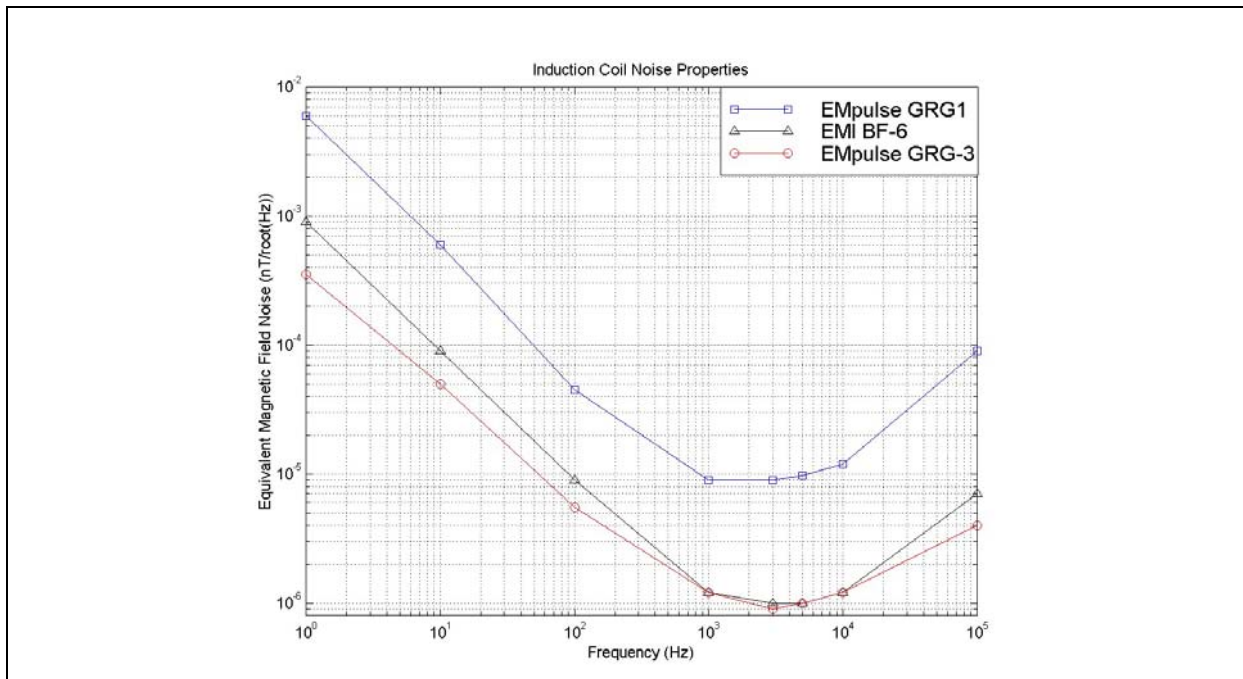


Figure 8. Induction coil noise property curves.

The interpretation of a shallow lateral contact at approximately 100 m depth, with an abrupt eastern edge at 20W/21W (i.e., indicated by a TM mode undershoot with strong Ty tipper anomaly) and a more gradational western edge at 29W (i.e., indicated by a weak Tx anomaly, whilst there is no TM mode contact effect evident), and with a basement conductor in the vicinity of 23W/24W agrees very well with the interpretation of gravity data (Figure 9) and fixed loop UTEM III data (Figure 10).

The prominent residual gravity low, as large as 1.8 mGal, is present with width of the order of 800 to 1200 m. It is postulated to be due to a shallow source that is present in the sandstone and is interpreted to be associated with fracturing and/or alteration in the sandstone, possibly related to major north-south trending basement structure. Modelling of the Bouguer gravity data on line WAS-4 indicates that the depth to the top of the body is less than 200 m, and that the source of the gravity low is a wedge that is tapered at depth. The eastern boundary of the edge is generally steeper compared to the western edge (pers. comm., Mr. Rod Koch). Reflection seismic data collected on WAS-4 also shows an anomalous zone of highly fragmented reflectivity over this lateral interval (pers. comm., Dr. Z. Hajnal).

Modelling of UTEM III fixed loop data indicates a basement conductor with 32 S conductance at a depth of 700 to 800 m, located at 2350W (Craven et al., 2007). Note the migration of the peak in the  $H_x$  component from 19W/20W at early time to approximately 2350W/24W at late time (Figure 10). The early time peak at 19W in the UTEM III data would appear to be a response to the steep eastern contact of the presumed wedge like conductive body in the sandstone.

The only puzzling part of the integrated picture is that DC resistivity data and VLF-R collected on WAS-4 (Figure 10). These do not appear to be in agreement with the other data sets with respect to the interpreted shallow sandstone structure/alteration. Despite the use of a moving Schlumberger array with a current electrode spacing of 300 m and MN/2 of 25 m, there is no evidence of a shallow resistivity anomaly between 29W and 21W. Instead, there is a resistivity low of 1000  $\Omega$ m much further to the east, in the vicinity of 4W. The resistivity low seen in the 'transient' AMT data, and partially with the conventional AMT data, between stations 21W and 29W, is of the order of 300  $\Omega$ m or less, and this agrees with the resistivity values typically associated with clay alteration zones in the sandstone.

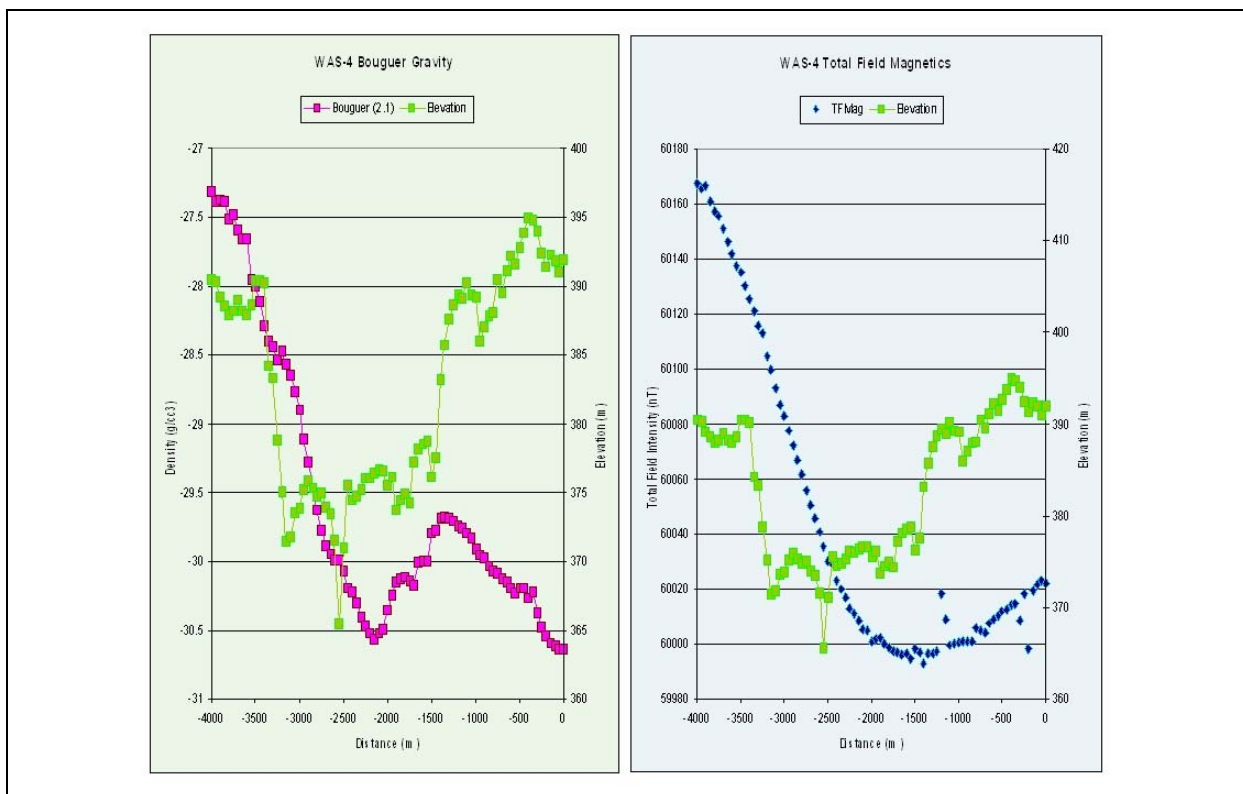


Figure 9. Bouguer gravity, total field magnetic and elevation profiles for line WAS-4.

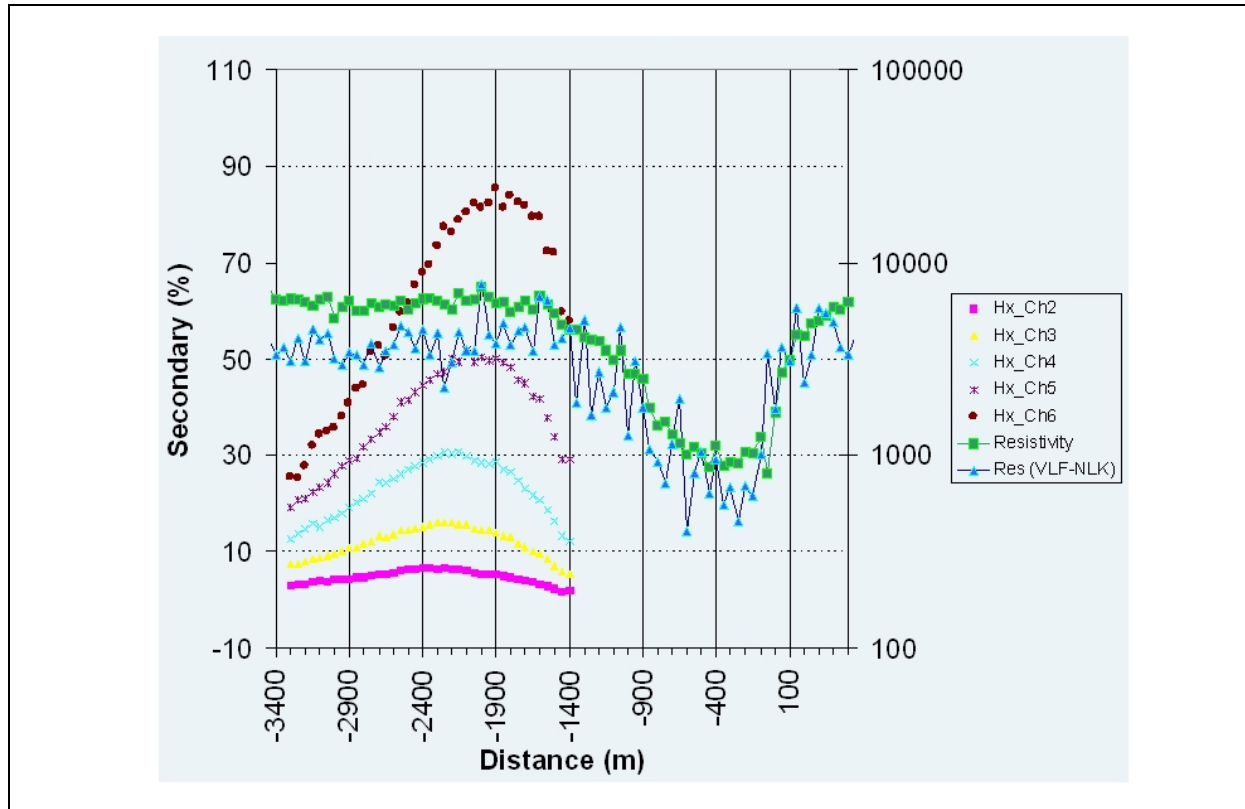


Figure 10. UTEM fixed loop Hx, DC resistivity, and VLF resistivity profiles for line WAS-4.

## Conclusions

The effectiveness of our 'transient' approach to AMT with Adaptive Polarization Stacking algorithm has been demonstrated through a direct comparison with 'conventional' AMT with robust remote-reference analysis.

Despite using coils that were approximately ten times noisier above 1000 Hz and approximately 4 times noisier below 100 Hz, and an ADC driver software bug that resulted in the removal of all the pre-trigger data, the APS impedance estimates are arguably as good as the conventional estimates and the APS tipper estimates are clearly better in our opinion.

This would appear to be due to the localization of large amplitude transients and SNR enhancement through our time domain stacking process that takes proper accounting of their polarization and sample size. It should be noted that our recording times of 20 minutes (15 minutes effectively) were considerably longer than the 7 minutes used in the conventional AMT survey for sub-1000 Hz data and 7 s for data greater than 1000 Hz.

The largest enhancements with respect to impedance are seen at high frequency where the APS estimates better map shallow alteration features in the sandstone, although the westerly dip of graphitic metasediments in the basement is also better seen in the TE mode APS estimates. The rather large difference in the TM mode phases of the two systems remains unexplained however.

Our tipper data appear to be better across the entire bandwidth, being smoother and more self-consistent at both low and high frequency. They more clearly reveal the response for the Saskatoon Lake conductor at approximately 23W ( $T_y$ ) and the shallow contacts at approximately 20W/21W ( $T_y$ ) and 29W ( $T_x$ ). Secondary resonance issues, which destroyed the high frequency impedance phase estimates, had less of an effect on the tipper, presumably due to partial cancellation of the effect when taking the ratio of two coil responses.

Most importantly, our 'transient' AMT data integrates very well with what is known about the geology in the area of line WAS-4. The westerly dip of graphitic metasediment gneiss is clearly seen in our TE

mode resistivity data, the Saskatoon Lake conductor at 2350W is evident in our impedance but especially the tipper data ( $T_y$ ). Shallow structure with a sharp eastern edge and a more gradational western edge is clearly apparent in the TM impedance and the tipper. This corroborates very well the previous, completely independent, interpretation of gravity data collected on WAS-4.

In order to obtain the best possible Earth response curves, especially outside the continuing 'windows', the use of transients to maximize SNR is mandatory. Whether one field records them in a time-localized fashion or streams data to disk continuously and searches for them after the fact, is not really important. What matters most is that recording take place for a long enough time to receive enough events from as many different directions as possible and an algorithm such as APS is used to properly locate and process the transients. If using RR, Monte Carlo simulation would be required to obtain more realistic error bars, as we do with APS, due to non-circularity of the source field.

The collection of a larger data set with one set of equipment would provide a common time series that would enable a better comparison of the performance of robust RR with APS. Most conventional AMT recordings, at least at high frequency, are too short for proper application of the APS method.

Along similar lines, we are working towards testing the BIRRP code (Chave and Thomson, 2004) with respect to bias and error bar capture in order to compare with APS. This is done via Monte Carlo simulation whereby a pool of many hundreds of real magnetic field events is used to create the perfectly matching electric field events assuming a known 3D impedance and tipper. The perfect relation between electric and magnetic fields is then perturbed with Gaussian noise of some level, a chosen number of noisy events are randomly selected out of the pool of events, and an impedance and tipper estimated. The result is stored and repeated many thousands of times. In this fashion, the level of bias and error bar performance of APS (already completed) and BIRRP could be compared.

## References

- Barr, R., 1970, The propagation of ELF and VLF radio waves beneath an inhomogeneous anisotropic ionosphere: *Journal of Atmospheric and Terrestrial Physics*, 33, 343-353.
- Chave, A. D., and Thomson, D. J., 2004, Bounded influence estimation of magnetotelluric response functions: *Geophysical Journal International*, 157, 988-1006.
- Craven, J. A., McNeice, G., Powell, B., Koch, R., Annesley, I. R., Wood, G., Mwenifumbo, C. J., Unsworth, M. J., and Xiao, W., 2007, Audio Magnetotelluric studies at the McArthur River mining camp and Shea Creek area, northern Saskatchewan; In Jefferson, C.W. and Delaney, G. (ed.), EXTECH IV: Geology and Uranium EXploration TECHnology of the Proterozoic Athabasca Basin, Saskatchewan and Alberta: Geological Survey of Canada, Bulletin 588 (also Saskatchewan Geological Society, Special Publication 18; Geological Association of Canada, Mineral Deposits Division, Special Publication 4), 413-424.
- Garner, S. J., and Thiel, D. V., 1999, Broadband (ULF-VLF) surface impedance measurements using MIMDAS: *Exploration Geophysics*, 31, 71-76.
- Goldak, D. K., and Goldak, M. S., 2001, Transient magnetotellurics with adaptive polarization stacking: SEG, Expanded Abstracts, 20, 1509-1512.
- Grillot, L. R., 1975, Calculation of the Magnetotelluric Tensor Impedance: Analysis of Band Limited MT Signal Pairs: *Geophysics*, 40, 790-797.
- Hajnal, Z., White, D. J., Takacs, E., Gyorfi, I., Annesly, I. R., Wood, G., O'Dowd, C., and Nimeck, G., 2010, Application of modern 2-D and 3-D seismic reflection techniques for uranium exploration in the Athabasca Basin: *Canadian Journal of Earth Sciences*, 47, 761-782.
- Kosteniuk, P. R., and Paulson, K. V., 1988, The application of polarization stacking to natural source magnetotellurics: Paper presented at the Annual Meeting of the Canadian Geophysical Union.

- Larsen, J., Mackie, R. L., Manzella, A., Fordelisi, A. and Rieven, S., 1996, Robust smooth magnetotelluric transfer functions: *Geophysical Journal International*, 124, 801-819.
- Hoover, D. B., Frischknecht, F. C. And Tippens, C. L., 1976, Audio-magnetotelluric sounding as a reconnaissance exploration technique in Long Valley, California: *Journal of Geophysical Research*, 81, 801-809.
- Kotaki, M., and C. Kato, 1983, The global distribution of thunderstorm activity observed by the Ionospheric Sounding Satellite (ISS-b): *J. Atmos. Terr. Phys.*, 45, 843-847.
- Leppin, M., and Goldak, D., 2005, Mapping deep sandstone alteration and basement conductors utilizing audio magnetotellurics: Exploration for uranium in the Virgin River area, Athabasca Basin, Saskatchewan, Canada: *SEG, Expanded Abstracts*, 24, 591-594.
- Nimeck, G., and Koch, R., 2008, A progressive geophysical exploration strategy at the Shea Creek uranium deposit: *The Leading Edge*, 27, 52-63.
- Powell, B., Wood, G., and Bzdel, L., 2007, Advances in Geophysical Exploration for Uranium Deposits in the Athabasca Basin: In B. Milkereit (ed.), *Proceedings of Exploration 2007, Fifth Decennial International Conference on Mineral Exploration*, 771-790.
- Tzanis, A., and Beamish, D., 1987, Audio-magnetotelluric sounding using the Schumann resonances: *Journal of Geophysics*, 61, 97-109.
- Vozoff, K., 1991, The magnetotelluric method: In *Electromagnetic methods in applied geophysics – Applications* (edited by M. Nabighian), *Society of Exploration Geophysicists*, 641-711.